

ARTICLE

Neutronic Analysis of the KRUSTY Space Microreactor

Shady ELSHATER^{1,2*}, Alexey CHEREZOV¹, Annalisa MANERA^{1,2},
Alexander VASILIEV¹ and Hakim FERROUKHI¹

¹ Laboratory for Reactor Physics and Thermal-Hydraulics, Paul Scherrer Institute (PSI), Villigen, Switzerland

² Department of Mechanical and Process Engineering, ETH Zurich, Zurich, Switzerland

Space microreactors are possibly the only option capable of providing reliable power to the future colonies on the Moon or Mars or to electric space propulsion systems. A concept with a lot of literature is the KRUSTY reactor designed and tested by Los Alamos National Laboratories. As part of a wider project on space microreactors at Paul Scherrer Institute, and in preparation for further extended studies, the core and shielding's neutronic analysis of the KRUSTY reactor was performed using Serpent, which showed good agreement with the data published by Los Alamos. This work was limited to the "hot" reactor condition used in the KRUSTY reports, where all components are at 300K.

KEYWORDS: microreactor, reactor, heat pipe, space, Krusty, neutronic, core, shielding, Serpent

I. Motivation

The *newspace* age is driving renewed interest in nuclear fission systems for space applications. These systems offer reliable power for surface missions on the Moon and Mars, as well as nuclear electric propulsion (NEP) for deep space missions. Space microreactors differ from terrestrial reactors due to their compact size, fast neutron spectrum, and high neutron leakage rates, making their neutronic behavior much less commonly benchmarked compared to thermal or large fast reactors.

The KRUSTY, short for Kilowatt Reactor Using Stirling Technology¹⁾ microreactor, developed by NASA's Kilopower project, is one of the few systems with publicly available neutronic results, also validated by real system tests. This study uses KRUSTY as a benchmark to evaluate the Monte Carlo code Serpent for high-leakage, fast-spectrum reactors, helping to validate its application for future nuclear space systems.

II. Introduction

KRUSTY was the continuation of the Kilopower project initiated in 2015 by NASA and the Department of Energy. It also marked the first demonstration of space-based fission power technology in over 50 years. The project was deemed highly successful and stands out for several reasons:

- It used heat pipes, a design scalable to higher power levels, as seen in advanced microreactors like eVinci, Aurora, and MARVEL.
- Its small size made it affordable, with the development costing \$18 million over approximately 3.5 years.
- Its extensive data is available in contrast with older reactors, such as TOPAZ-1.

Table 1. Main KRUSTY specifications

Specification	Unit	Value
Thermal power	kWt	4.3-5
Fuel		
Spectrum		Fast
Enrichment U-235	%	93.1
Mo content	%	7.65
Fuel total mass	kg	32.2
Fuel length	cm	25
Fuel out/in diameter	cm	11 / 4
Fuel density	g/cm ³	17.34
Heat pipes		
Material		Haynes 230
Amount		8
Coolant		Sodium (Na)
Na content	g	15
Length	cm	100
Outer diameter	cm	1.27
Wall thickness	cm	0.089

The broader *Kilopower* program envisioned reactor sizes ranging from 1 to 10 kWe (4.3 to 43 kWt) with heat pipe counts from 8 to 24. While concept designs for the flight version were proposed during the initial *Kilopower* studies, KRUSTY itself was solely a test reactor. It lacked lightweight components, detailed radiator designs, and operational systems for flight. The proposed flight concept had an estimated mass of 327–390 kg. Additionally, reactivity control differed from the flight concept, relying on the motion of the radial reflector platform instead of the 96%-enriched B-10 B₄C control rods. The main specifications and details are listed in **Table 1**.

*Corresponding author, E-mail: shady.elshater@gmail.com

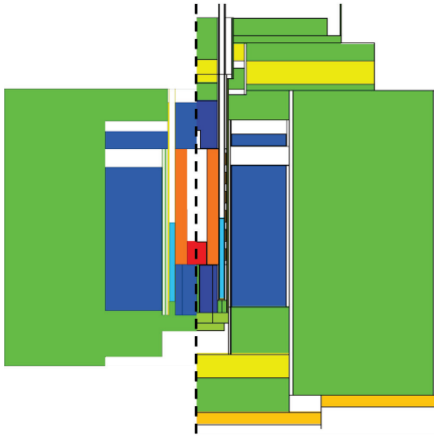


Fig. 1 Comparison between our KRUSTY CAD model (left) and the one used by the KRUSTY development team for MCNP6 (right, ²). The *Serpent* model clearly presents fewer details.

II. Design

The detailed design of KRUSTY has been extensively covered in existing literature.¹⁾ For the present simulations, KRUSTY's geometry was constructed from scratch as a 3D CAD model and exported as an STL file, as no pre-existing models were publicly available. This process meant that certain design elements were omitted. For instance, the six clamps around the fuel, slightly visible on the right side of **Fig. 1**, were not included in the CAD model.

Additionally, some component measurements, unavailable in reports, had to be inferred from images. Despite these adjustments, minor discrepancies remain. For example, slight variations in component dimensions and missing details, such as the interaction between the fuel and reflectors, might contribute to differences in simulated outcomes.

These simplifications highlight the trade-offs necessary when building reactor models for computational analysis.

Table 2 KRUSTY materials used in Fig. 1

Component	Material	Color
Fuel	U-8Mo	Orange
Reflector	BeO	Blue
Absorber rod	B4C (¹⁰ B-enr.)	Red
Heat pipe medium	Na	Turquoise
Outer structure	SS316	Green
Extra absorbers	B4C	Yellow
Extra structures	Al	Light orange

III. Results

In all KRUSTY reports, two reactor conditions are defined:

- Cold: all components have a temperature of 300K
- Hot: all components have a temperature of 300K, except for the fuel, which is at 1'000K.

All the results presented assume a cold status since this was also done for the results in the KRUSTY reports that are being compared with. The only exception is the fuel temperature reactivity, where the temperature of the fuel was increased in order to study the change in reactivity.

The number of cycles and neutron histories per cycle used in the *Serpent* models varied depending on the simulation.

Depending on which and how many detectors (energy spectrum, power distribution, dose, etc.) were active, more or fewer cycles could be used in order not to make the simulation excessively long (due to the computational demand).

A typical run had between 1'000 and 2'000 cycles and a neutron population of 200'000 – 500'000, with one simulation reaching the 1 million mark. A typical run (2'000 cycles and 500'000 neutrons) had the reactor in cold state, a control rod height of 0 cm (which was standard since the control rod was not used for active control, but its base was still always fully inserted), and a fully loaded reflector (12"), which would result in an analog keff of 1.013985 with a relative statistical error of 0.0041% and a β eff (IFP method) of 0.00692958 with a relative statistical error of 0.169%. The KRUSTY design and modeling report³⁾ listed an "all cold" keff of 1.01288 and a β eff of 0.0069 for this reactor configuration. The difference of 16 cents is smaller than the difference of around 18 cents when using the cross-section library ENDF7.1 instead of ENDF7.0, which was used for the KRUSTY reports as well as in this work.

1. Spectrum

The distribution of fission reaction rates across energy groups, binned by lethargy intervals, obtained through *Serpent* simulations is highly consistent with the one provided in the KRUSTY reports. The plot in **Fig. 2** reveals a small peak in the thermal energy region, with most fissions occurring within the 0.1 to 10 MeV range.

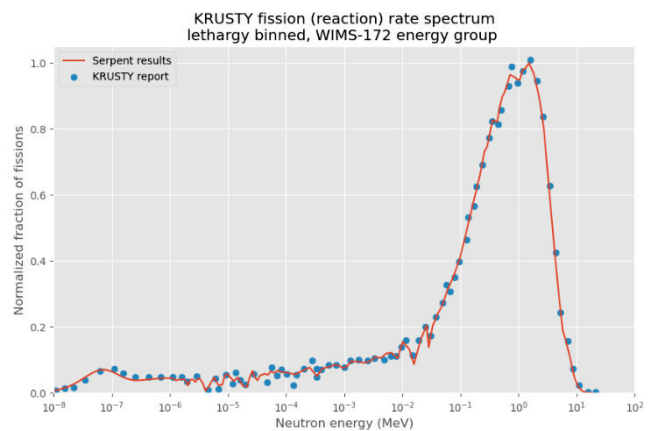


Fig. 2 Fission (reaction) rate spectrum comparing *Serpent* results with a few data points normalized from the KRUSTY report.³⁾

2. Power Distribution

The power distribution shows edge heating along the outer perimeter, where the holes of the 8 heat pipes are also visible. KRUSTY's small core and hard neutron spectrum result in a nearly flat internal power distribution. However, power peaks at the axial and radial edges arise due to the BeO reflector's strong neutron moderation, which increases fission reaction rates by reflecting low-energy neutrons back into the fuel, as also noted in Refs. 1) and 3)

The axial peaks are much more visible when examining the full axial power distribution, shown in **Fig. 4**, especially at the bottom of the fuel (axial position of 0 cm in the plot). The bottom peak is noticeably higher than reported, potentially

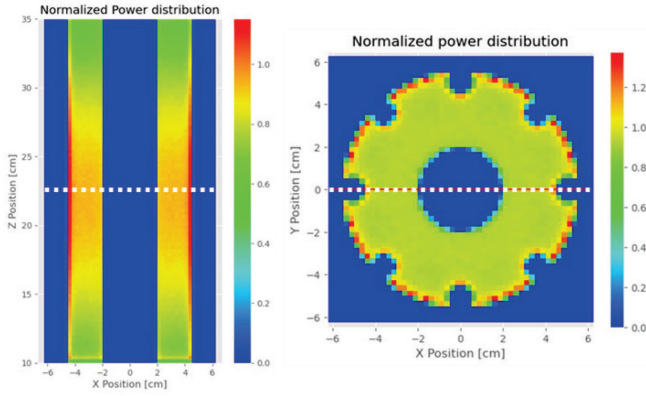


Fig. 3 Normalized power distributions of a longitudinal (left) and of a circumferential (right) section. The positions of the two cuts are marked with the dotted white line.

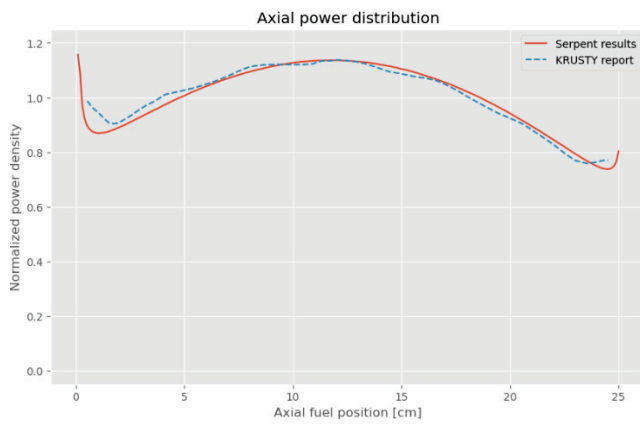


Fig. 4 Axial power distribution

because the KRUSTY report's plot covered only 24 cm of length, effectively omitting 0.5 cm from each end.

The overall axial peaking factor is reported as 1.15 in the KRUSTY documents, while Serpent simulations show a slightly higher maximum factor of 1.157, excluding boundary effects. This value is relatively small compared to most reactors. KRUSTY's low axial peaking factor likely results from its high L/D ratio and the fast neutron spectrum, which increases the mean free path of neutrons relative to the core's small length.

Additionally, the KRUSTY report identifies five small bumps in the axial power distribution caused by fuel clamps, which are absent in the Serpent CAD model. This omission may explain differences in localized power distributions.

3. Fuel Temperature Reactivity

Two primary factors influence reactivity when fuel temperature rises: thermal expansion and changes in cross sections. In a fast reactor like KRUSTY, which uses U-8Mo fuel known for significant swelling at elevated temperatures, thermal expansion is the dominant factor, responsible for over 90% of the reactivity decrease.¹⁾ The KRUSTY report indicates that changes in cross sections contribute only minimally to the overall reactivity reduction. If KRUSTY were redesigned with moderated HALEU fuel,⁴⁾ the cross-

section feedback would likely increase due to a higher proportion of U-238, which absorbs more in the resonance region.

The result obtained with Serpent (considering both cross-section and expansion effects) shows an even larger reactivity

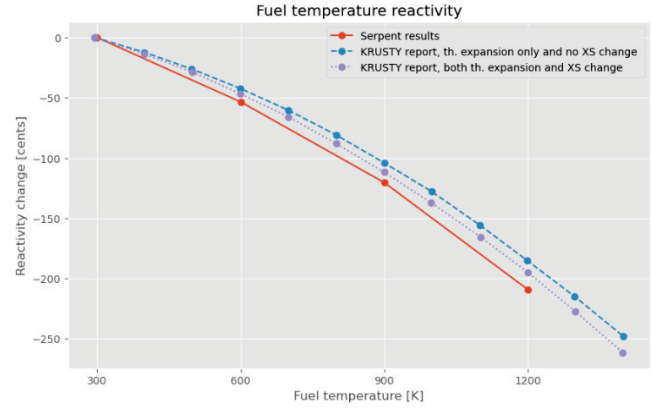


Fig. 5 Fuel temperature reactivity

decrease (14 cents less than the KRUSTY report at 1'200K), as shown in **Fig. 5**. To understand the possible reasons, it is necessary to explain how these simulations were set up, knowing that it was decided to run them with fuel temperature at 300 (standard cold status), 600, 900, and 1'200K:

Cross sections: The ENDF/B-7.0 library, also used in the KRUSTY report,³⁾ was employed, ensuring no discrepancies from this source.

Thermal expansion: Expansion affects both the geometry, as the fuel grows larger, and its density, which decreases. There are two approaches to account for the thermal expansion effect: using the temperature-density relationship for U-7.65Mo or employing the linear thermal expansion coefficient as a function of temperature. The latter approach can be expressed mathematically as

$$\frac{\rho(T_0 = 300K)}{\rho(T)} = (1 + \epsilon_{lin}(T))^3 = (1 + \alpha(T) \cdot (T - T_0))^3 \quad (1)$$

where ϵ_{lin} is the linear material strain at a certain temperature, which is calculated as the multiplication of the integral linear thermal expansion coefficient $\alpha(T)$ with the change in temperature ΔT . One also needs to check if $\alpha(T)$ is provided as an instantaneous or integral coefficient of thermal expansion. The thermal expansion coefficients were obtained from the quadratic formula provided in an IAEA document,⁵⁾ and they refer to U-7.18Mo. Unfortunately, the KRUSTY report, which provided the integral coefficients as a plot for U-8Mo,³⁾ was only found at a later stage, without enough time to re-run all simulations with them. Nevertheless, the coefficient corresponding to the IAEA report used (referring to U-7.18Mo) and the one from the KRUSTY report (U-8Mo) can be compared as done in **Fig. 6**.

As expected, the values used present a greater strain, which is compatible with the larger decrease in reactivity. Further, it also makes sense that the strain of U-7.18Mo is larger than

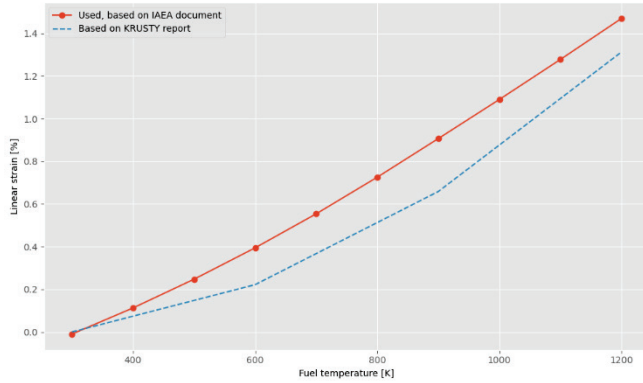


Fig. 6 Comparison of total linear strain between values used and KRUSTY report.

that of U-8Mo, due to the lower concentration of Mo (effect also observable in the IAEA report⁵⁾ for Mo concentrations between 7.18 and 12.10%). More time should be spent investigating which of the two models better corresponds to the actual material behavior, which has a Mo concentration of 7.65%.

Another consideration is the method of applying expansion. The KRUSTY design report³⁾ states that most components expand freely, with specific interference rules hardcoded for some interactions. However, no detailed rules are provided. In this study, the fuel block was expanded radially and longitudinally based on strain, without altering the positions of heat pipes. This approximation does not replicate the physical forces between the heat pipes and fuel, potentially contributing to differences in reactivity outcomes.

The observed 14-cent discrepancy underscores the importance of precise thermal expansion modeling and multi-physics tools. For comparison, switching between cross-section libraries ENDF/B-VII.0 and ENDF/B-VII.1 caused an 18-cent reactivity increase, further illustrating the significant impact of these parameters on results.

4. Control Rod Worth

As previously noted, KRUSTY's reactivity control was achieved by adjusting the entire radial reflector platform rather than moving the B4C absorber rod. However, since the flight version is expected to include a central control rod, a

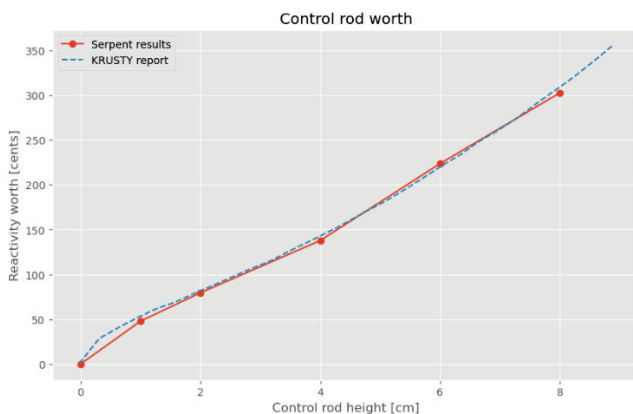


Fig. 7 Control rod worth

fixed-length B4C rod (ranging from 0 cm, representing no control rod, to 12 cm) was used in simulations to evaluate its reactivity worth. The results are shown in **Fig. 7**. While the maximum theoretical rod length was approximately 12 cm, the KRUSTY report provided data for rod lengths up to 9 cm.

The Serpent simulation results showed good agreement with the KRUSTY report. Additional tests were conducted to analyze reactivity changes as a function of rod position using a control rod fixed at a maximum length of 12.5 cm. Unfortunately, corresponding simulations for this setup were not documented in the available KRUSTY reports.

5. Reflector Height and Gap

KRUSTY could hold a maximum reflector height of 12", plus an additional 2" of so-called shim reflector fixed directly to the upper structure. The heights of moving and shim reflectors loaded could be changed between tests, while the vertical position of the moving reflector was used for reactivity control during each test. As the platen was moved up, the gap between shim and moving reflector closed, and the reactivity increased. In **Fig. 8**, the reactivity as a function of reflector height, assuming no shim reflector and a fully raised platen, is compared. The plot goes up to a reflector height of 12", which corresponds to the maximum height that could be loaded on the moving platen.

Other than the reflector height, the reactivity as a function



Fig. 8 Criticality as a function of reflector height, assuming a fully inserted platen and no shim reflector.



Fig. 9 Criticality as a function of reflector gap

of the platen position can also be studied. With a shim reflector and with a fully loaded radial moving reflector, the position of the platen defines the reflector gap, which is the gap between the shim and the moving radial reflector. The results of the criticality as a function of reflector gap are shown in **Fig. 9**.

The KRUSTY report and Serpent results agree once again, with the interesting value being the crossing of the criticality ($k_{eff} = 1$) at a reflector gap of 2.2cm in the KRUSTY report and of 2.45cm in the Serpent simulations.

6. Shielding

The shielding design for the flight version was mostly part of the preliminary studies of the *Kilopower* team and not so much during the KRUSTY development and testing. In this sense, KRUSTY had a very thick and heavy stainless-steel wall all around the core, mainly meant to protect personnel during testing. The shielding of a flight reactor, for example, for a NEP (Nuclear Electric Propulsion) spaceship would only need to protect the other components of the NEP system (power conversion, radiators, payload, etc.) from the radiation emitted by the core.

For this, a typical shield cone is used. While some *Kilopower* reports mentioned different target dose levels (e.g. “tight” and “relaxed”) measured at planes 10 or 15 m behind the shielding, the report with the most details about the shielding design⁶⁾ provided upper limits for neutron fluxes and photon hourly doses right behind the shield. Hence, the latter, whose shielding design is shown in **Fig. 10**, was used as a benchmark.

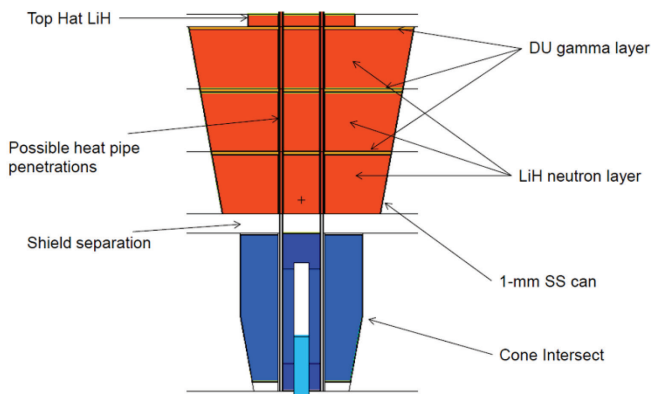


Fig. 10 Kilopower 1kW_e (4kW_{th}) flight concept shielding⁶⁾

The shielding featured depleted uranium (DU) as high-Z material for photon absorption and lithium hydride for neutron absorption. The thermal power assumed for the simulations was 4.3 kW_{th}. In the custom CAD model built to be used with Serpent, the design was again slightly simplified, and, for example, only one DU layer with a thickness equal to the sum of the three DU layers shown in Figure 10 was used (2.25 cm instead of 3 times 0.75 cm).

The summary of the results obtained with Serpent compared with the ones from the *Kilopower* report is shown in **Table 3**.

Table 3 Comparison of neutron fluence and photon doses

	Neutron		Photon	
	Flux 10 ⁵ n/cm ² s	Fuence (15yr) 10 ¹⁴ n/cm ²	Hourly dose rad/hr in Si	Total dose (15yr) Mrad in Si
<i>Serpent</i> (avg.)	0.54 ± 0.03	0.26 ± 0.02	49.08 ± 0.2	6.4 ± 0.03
<i>Serpent</i> (centerline)	4.275 ± 0.28	2.02 ± 0.13	-	-
<i>Kilopower</i> ⁶⁾	< 2	< 1	< 40	< 5

While the *Kilopower* report did not provide precise figures, one can still compare the orders of magnitude, which are very similar. The Serpent results show an average neutron flux behind the shield that is lower than the target limit. However, the peak neutron flux at the centerline (which is, however, a value that is much more dependent on statistics due to the MC method used) would be above that limit.

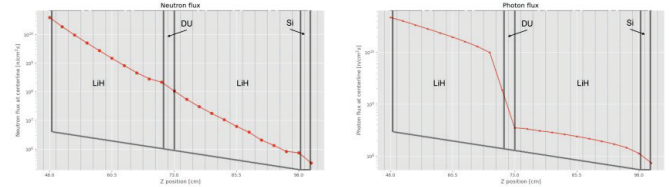


Fig. 11 Left: Neutron flux through the shield, with continuous intensity decrease through the LiH layer. Right: Photon flux through the shield, with a clear intensity drop through the high-Z DU layer.

In terms of photon hourly dose as Rad/hr in Si, the average behind the shield is slightly higher than the *Kilopower* report, which sets an upper limit at 40 rad/hr in Si.

As a final step, one can also compare the neutron flux qualitatively, as shown in **Fig. 12**, where the two appear very similar.

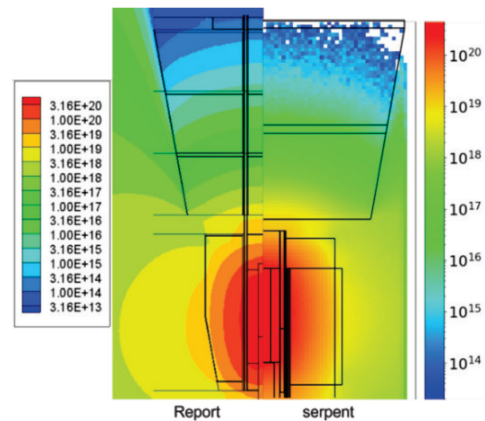


Fig. 12 Comparison of neutron flux through shielding of *Kilopower* report⁶⁾ and from Serpent results

III. Conclusion

The neutronic simulations run with Serpent show very similar results to the various KRUSTY reports generally run with MCNP. Many characteristics were compared, starting with spectrum and power distributions and then moving towards reflector and control rod worth, as well as shielding

design. Some of the other simulations run included burnup calculations, but these were not included in this work since there was no data in literature to compare them to.

As mentioned at the start of this work, the two “hot” and “cold” reactor conditions were used for direct comparisons with the KRUSTY reports, since only those were provided. However, these conditions do not reflect the real reactor conditions, which would instead present significant three-dimensional temperature distributions due to the fuel as the heat source and the sodium heat pipes as the main heat sink. These distributions would then also affect the thermal expansion of each material, and as a consequence, density, geometry, and last but not least, the stress inside the different components. All these phenomena have to be accounted for in a proper and extensive multi-physics coupled analysis of KRUSTY. Further, many additional aspects, such as irradiation creep, which is significant for metallic fuels, the overall burnup throughout the reactor lifetime, as well as the very critical transient phases at startup and shutdown, should be considered too. Unfortunately, data for all these points is not available in the KRUSTY reports. This would hence require a separate evaluation, which was beyond the scope of this work, which mainly focused on comparing the available literature data.

The next steps for completion of the presented verification

studies would be to refine the 3D models to include more details, rerun the fuel temperature reactivity calculations with the exact same material properties, and finally start with multi-physics simulations as well as consider the use of deterministic codes instead of only MC-based ones.

References

- 1) D. I. Poston, M. A. Gibson, T. Godfroy, P. R. McClure, “KRUSTY Reactor Design,” *Nuclear Technology*, **206(sup1)**, S13-S30, (2020).
- 2) P. R. McClure, D. I. Poston, S. D. Clement, L. Restrepo, R. Miller, M. Negrete, “KRUSTY Experiment: Reactivity Insertion Accident Analysis,” *Nuclear Technology*, **206(sup1)**, S43-S55 (2020).
- 3) D. I. Poston, “KRUSTY Design and Modeling”, *Technical Report LA-UR-16-28377*, 1330651, LANL, (2016).
- 4) L. De Holanda Mencarini, J. C. King, “Fuel geometry options for a moderated low-enriched uranium kilowatt-class space nuclear reactor,” *Nuclear Engineering and Design*, **340**, 122-132 (2018).
- 5) IAEA, “Material Properties of Unirradiated Uranium-Molybdenum (U-Mo) Fuel for Research Reactors.” *Number 1923 in TECDOC Series*, IAEA, (2020).
- 6) D. Poston, M. Gibson, P. McClure, J. Creasy, C. Robinson, C. Bowman, L. Mason, “Thermal power scaling of the kilopower space reactor.” (2015).